Modeling Cusps in Adiabatic Potential Energy Surfaces

ARTICLE *in* THE JOURNAL OF PHYSICAL CHEMISTRY A · JANUARY 2015

Impact Factor: 2.69 · DOI: 10.1021/jp512671q · Source: PubMed

3 AUTHORS, INCLUDING:

Breno Galvão
Centro Federal de Educação Tecnológica de M…
16 PUBLICATIONS **73** CITATIONS
SEE PROFILE

Antonio J. C. Varandas
University of Coimbra
382 PUBLICATIONS **6,750** CITATIONS
SEE PROFILE

THE JOURNAL OF PHYSICAL CHEMISTRY A

Article

pubs.acs.org/JPCA

Modeling Cusps in Adiabatic Potential Energy Surfaces

B. R. L. Galvão,*[,†] V. C. Mota,*[,‡] and A. J. C. Varandas*[,§,‡]

[†]Departamento de Química, Centro Federal de Educação Tecnológica de Minas Gerais, CEFET-MG, Av. Amazonas 5253, 30421-169 Belo Horizonte, Minas Gerais, Brazil

[‡]Departamento de Física, Universidade Federal do Espirito Santo, Av. Fernando Ferrari 514, 29075-910 Vitória, Brazil

[§]Departamento de Química and Centro de Química, Universidade de Coimbra, 3004-535 Coimbra, Portugal

ABSTRACT: A method for modeling cusps on adiabatic potential energy surfaces without the need for any adiabatic-to-diabatic transformation is presented and shown to be successfully applied to the $^2A''$ state of NO_2. The more complicated case of a system with permutationally equivalent crossing seams is also examined and illustrated by considering the two first $^2A'$ states of the nitrogen trimer.

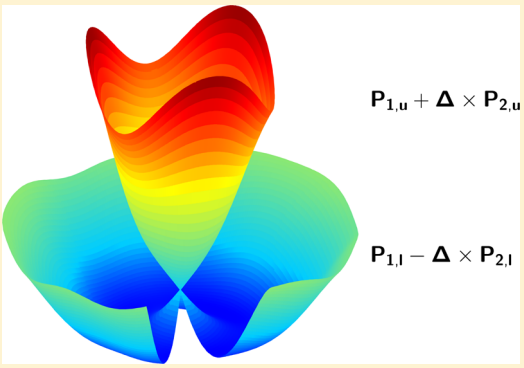

INTRODUCTION

It is well known that the modeling of potential energy surfaces (PESs) is often drastically complicated by the presence of conical intersections. Along the crossing seam, the two degenerate electronic states form a double cone in the 2D space orthogonal to the seam. Thus, each adiabatic state shows a cusp and presents a discontinuous first derivative, which cannot be modeled by analytic functions.

To circumvent this problem, a diabatic matrix representation is often employed in which the elements are smooth functions of the molecular geometry and which can be diagonalized to yield the adiabatic states, including the cusps. There are many approaches to the fitting of such smooth diabatic states, with a relatively recent review given elsewhere by two of the authors.[1] (See also a more recent paper[2] from which further references may be obtained via cross-referencing.) Of relevance for the present work are two main approaches: One starts from ab initio energies that are first diabatized and then fitted to a convenient analytic form;[1] the other[3] starts from a semi-empirical diabatic-type formalism such as LEPS[4−6] or the diatomics-in-molecules (DIM)[7−9] theory, which has built-in the cusps, and introduces additional terms to accommodate as much as possible the flexibility to fit ab initio data.

Besides being complicated, diabatization is not a unique process. Indeed, strictly diabatic PESs do not exist.[10] Thus, one may speak at most of "quasi-diabatic" PESs, and it is in this broad sense that they are to be understood.

To the best of our knowledge, the first functional form to model a cusp without resorting to diabatic representations is due to Porter, Stevens, and Karplus[11] for the H_3 PES. The electronic state of this molecule is doubly degenerate for D_{3h} arrangements, and hence the PES shows a symmetry-dictated conical intersection at such geometries. In fact, ground-state H_3 provides the best known example of a Jahn−Teller-type system.

Let now $\mathbf{R} = \{R_1,R_2,R_3\}$ be the vector formed by the three bond distances of a triatomic molecule. They can be transformed into symmetry-adapted coordinates as[12]

$$\begin{pmatrix} Q_1 \\ Q_2 \\ Q_3 \end{pmatrix} = \begin{pmatrix} \sqrt{1/3} & \sqrt{1/3} & \sqrt{1/3} \\ 0 & \sqrt{1/2} & -\sqrt{1/2} \\ \sqrt{2/3} & -\sqrt{1/6} & -\sqrt{1/6} \end{pmatrix} \begin{pmatrix} R_1 - R_0 \\ R_2 - R_0 \\ R_3 - R_0 \end{pmatrix} \quad (1)$$

where Q_1 is related to the perimeter of the triatomic and (Q_2,Q_3) are the other two that define the shape of the molecular triangle. Thus, for equilateral triangles: $Q_2 = Q_3 = 0$. Porter and coworkers[11] have shown that the H_3 PES could be modeled by employing the polar coordinate q_r defined by

$$Q_2 = q_r \cos\theta$$
$$Q_3 = q_r \sin\theta \quad (2)$$

and writing the upper (+) and lower (−) PESs as

$$V_\pm = A \pm q_r B \quad (3)$$

where $q_r = (Q_2^2 + Q_3^2)^{1/2}$ and A and B are polynomials expressed in terms of $\mathbf{Q} = \{Q_1,Q_2,Q_3\}$.

Clearly, it is q_r in eq 3 that causes the cusp on the PES at D_{3h} geometries, which led Varandas and Murrell[13] to use such a coordinate in modeling the lowest adiabatic PES of H_3. In fact,

Received: December 19, 2014
Revised: January 27, 2015
Published: January 29, 2015

DOI: 10.1021/jp512671q
J. Phys. Chem. A 2015, 119, 1415−1421

it can be used to model the conical intersection of any D_{3h} crossing seam, such as the one in ref 14, $N_3(^2A'')$. This coordinate is also part of the integrity basis,[15,16] which is useful for X_3 systems because it is totally symmetric

$$\Gamma_1 = Q_1$$
$$\Gamma_2^2 = Q_2^2 + Q_3^2$$
$$\Gamma_3^3 = Q_3(Q_3^2 - 3Q_2^2) \quad (4)$$

with $\Gamma_2 = q_r$.

Further progress on the use of eq 3 for modeling PESs has been made by Varandas and coworkers.[17] They have shown that it can be used not only to cause the cusp but also to fit simultaneously both ground- and excited-state sheets, hence ensuring degeneracy over the crossing seam while imposing the same slope for the upper and lower cones at the crossing. Note that it does not call upon the diabatic states and it has been the first approach to correctly mimic the two adiabatic sheets without so doing. In brief, the upper (u) and lower (l) surfaces are written as

$$V_u = V_u^{(2)} + V_{dc}^{(3)} + [P_{1,u} + \Gamma_2 P_{2,u}] \times T(\mathbf{R})$$
$$V_l = V_l^{(2)} + V_{dc}^{(3)} + [P_{1,l} - \Gamma_2 P_{2,l}] \times T(\mathbf{R}) \quad (5)$$

where, as inherent to the double many-body expansion (DMBE[18−22]) method, $V^{(2)}$ is the sum of two-body potentials, $V_{dc}^{(3)}$ is the three-body dynamical correlation term, $T(\mathbf{R})$ is a range-decaying factor, and the polynomials assume the general form

$$P_{(m,n)} = \sum_{i,j,k} c_{ijk}^{(m,n)} \Gamma_1^i \Gamma_2^{2j} \Gamma_3^{3k} \quad (6)$$

The two-body fragments must be equal on both sheets to make both adiabatic sheets degenerate along the D_{3h} line ($V_- = V_+$) (or forced to vanish at D_{3h} configurations[17]), and the u and l three-body terms must be the same at the crossing seam. Because both Γ_2 and Γ_3 are zero at D_{3h} configurations, it is seen from eq 5 that the only condition necessary to ensure degeneracy is that the coefficients of the polynomials P_1 that depend only on Γ_1 be the same: $c_{i00}^{(1,l)} = c_{i00}^{(1,u)}$, $\forall i$. Because eq 5 ensures that the two sheets behave as a linear function of the Jahn−Teller coordinate Γ_2 in the vicinity of the intersection seam (higher order terms are negligible there), the only additional constraint that must be imposed is to ensure the same slope: $c_{000}^{(2,l)} = c_{000}^{(2,u)}$.

Because all formalisms previously described deal with X_3 systems, we present here a simple, yet general, scheme to directly model cusps on adiabatic PESs and show by examples that it is not restricted to X_3-type systems. This is a very useful result because more realistic PESs can be developed for use in studies of both spectroscopy and reaction dynamics.

■ ALTERNATIVE APPROACH TO THE PROBLEM

In this work, we extend the previously described scheme to modeling cusps of conical intersections with other symmetries or even accidental ones. We start by noting that q_r is simply the distance from a given point to the intersection seam in the **Q** space,[11] with the intersection lying at $Q_2 = Q_3 = 0$, $\forall\, Q_1$. Next, we define the "distance" between the crossing seam and a point in **R** space. Because the **R** and **Q** coordinates are related by an orthogonal transformation (the norm of a vector is identical in both spaces), we consider the former because a general intersection can be more easily defined. As shown in Figure 1, the D_{3h} line is defined by the parametric line (t,t,t), where t is a dummy variable.

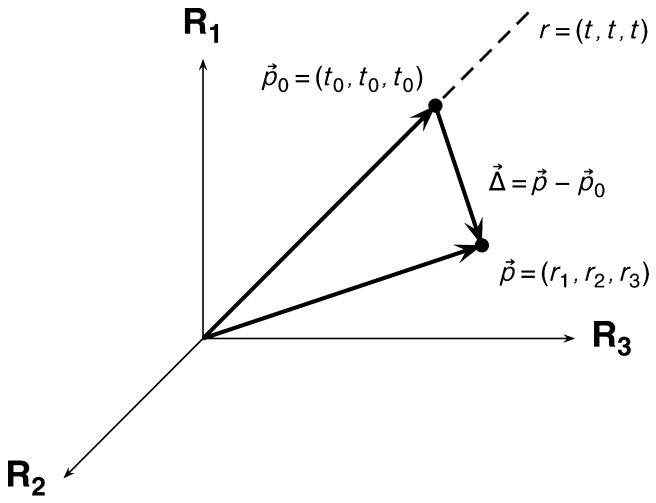

Figure 1. D_{3h} line in the **R** space and its distance from a given point.

Recall next that the value of the PES at a given point $\vec{\mathbf{p}} = (r_1,r_2,r_3)$ depends on its distance $\vec{\Delta}$ from the crossing seam [at $\vec{\mathbf{p}}_0 = (t_0,t_0,t_0)$], which is defined by

$$\vec{\Delta} = \vec{\mathbf{p}} - \vec{\mathbf{p}}_0 = (r_1 - t_0,\, r_2 - t_0,\, r_3 - t_0) \quad (7)$$

a vector whose norm is given by

$$\|\vec{\Delta}\| = \sqrt{(r_1 - t_0)^2 + (r_2 - t_0)^2 + (r_3 - t_0)^2} \quad (8)$$

The vector $\vec{\mathbf{p}}_0$ can then be obtained from the condition that $\vec{\Delta}$ is orthogonal to the seam

$$\vec{\Delta} \cdot \vec{\mathbf{p}}_0 = (r_1 - t_0)t_0 + (r_2 - t_0)t_0 + (r_3 - t_0)t_0 = 0 \quad (9)$$

which yields

$$t_0 = \frac{r_1 + r_2 + r_3}{3} \quad (10)$$

and

$$\|\vec{\Delta}\|^2 = (r_1 - t_0)^2 + (r_2 - t_0)^2 + (r_3 - t_0)^2 = \frac{2}{3}[r_1^2 + r_2^2 + r_3^2 - r_1r_2 - r_1r_3 - r_2r_3] \quad (11)$$

a result identical to q_r^2 in ref 11. As stated in the Introduction, this can be used to obtain cusped (discontinuous first derivative) functions that can correctly fit calculated ab initio energies. However, as it will be shown here, it can be readily extended to crossings other than the D_{3h} case, the only requirement being to find the parametric equation of the crossing. The final adiabatic potentials will then be obtained by using the distance $\vec{\Delta}$ from a point to the parametric line and an equation similar to eq 5

$$V_+ = V_+^{(2)} + V_{dc}^{(3)} + [P_{1,+} + \Delta P_{2,+}] \times T(\mathbf{R})$$
$$V_- = V_-^{(2)} + V_{dc}^{(3)} + [P_{1,-} - \Delta P_{2,-}] \times T(\mathbf{R}) \quad (12)$$

DOI: 10.1021/jp512671q
J. Phys. Chem. A 2015, 119, 1415−1421

Although all tests here performed employ DMBE[18−22] potentials, the approach to get $\vec{\Delta}$ is general and valid to create a cusp in any potential function, global or local.

APPLICATION TO $NO_2(1^2A'')$

As a first illustration, we use the approach to build a global accurate PES for $NO_2(1^2A'')$, which includes the correct description of the $^2A_2/^2B_1$ conical intersection over the entire seam. The first step consists of defining the parametric equation that locates the crossing seam. Because it occurs at geometries with C_{2v} symmetry,[23,24] it can be expressed in **R** space (R_1 is the O−O bond length) as $(f(t),t,t)$. For this purpose, we have performed ab initio cuts for geometries related to the T-shaped attack of the N atom to the OO diatomic and determined the point where the two involved adiabatic PESs cross each other. We have then mapped the crossing region, as shown in Figure 2, where it can be seen to be accurately represented by a

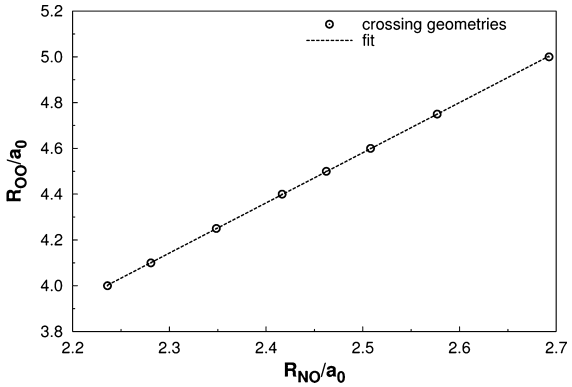

Figure 2. Location of the crossing seam at geometries with C_{2v} symmetry.

straight line. The seam of crossing is therefore defined by the parametric equation $(a + bt, t, t)$, with a and b determined from a fit to the calculated data; see Figure 2. In general, the crossing may assume a more complicated shape, but it can still be modeled in the same way to fit the available ab initio results.

The final step consists of calculating the distance from an arbitrary geometry to the crossing seam; see Figure 3. Using the same notation as above, it assumes the form

$$\|\vec{\Delta}\| = \sqrt{[r_1 - (a + bt_0)]^2 + (r_2 - t_0)^2 + (r_3 - t_0)^2} \tag{13}$$

with t_0 being now obtained from

$$\vec{\Delta}\cdot\vec{\mathbf{p}_0} = [r_1 - (a + bt_0)](a + bt_0) + (r_2 - t_0)t_0 + (r_3 - t_0)t_0 = 0 \tag{14}$$

One gets

$$t_0 = [r_2 + r_3 + br_1 - 2ab \pm [(r_2 + r_3 + br_1 - 2ab)^2 + 4(2 + b^2)(ar_1 - a^2)]^{1/2}] /[2(2 + b^2)] \tag{15}$$

which, upon substitution into eq 13, yields $\vec{\Delta}$. Note that, for $a \neq 0$, there will be two solutions for the above quadratic equation (one is obviously unphysical if negative, and hence should be discarded), but only the one that minimizes the distance of the point to the seam is to be considered.

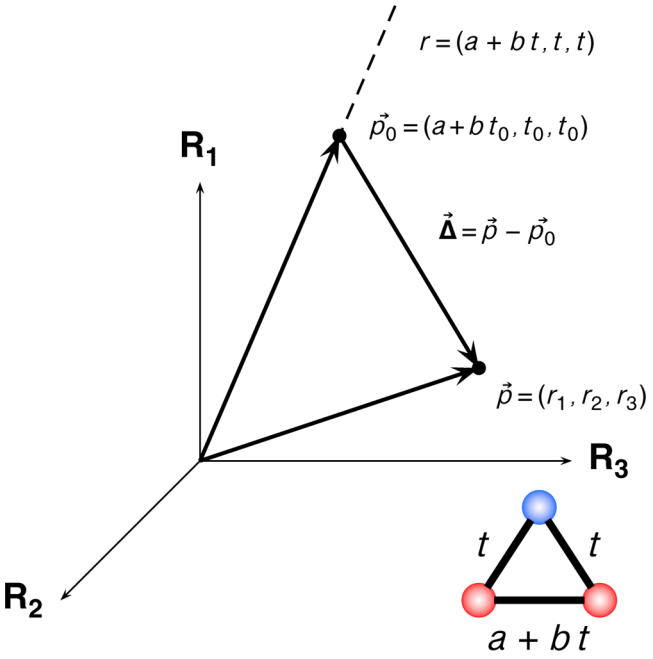

Figure 3. C_{2v} line and its distance from a given point.

We next illustrate the approach for the $1^2A''$ electronic state of NO_2. According to eqs 12 and knowing $\vec{\Delta}$, it is now possible to obtain the correct cusp for both electronic states in the vicinity of the $^2A_2/^2B_1$ crossing seam. For convenience, we focus here on the lowest adiabatic sheet for which accurate ab initio calculations are affordable and compare the results with previously reported fits.[24] The new global PES reported so obtained is compared with two distinct DMBE forms.[24] They are all based on

$$V(\mathbf{R}) = V^{(3)}(\mathbf{R}) + O_2(^3\Sigma_g^-)(R_1) + NO(^2\Pi)(R_2) + NO(^2\Pi)(R_3) + [N(^2D) - N(^4S)]\cdot f(\mathbf{R}) \tag{16}$$

where

$$V^{(3)}(\mathbf{R}) = V^{(3)}_{EHF}(\mathbf{R}) + V^{(3)}_{ele}(\mathbf{R}) + V^{(3)}_{dc}(\mathbf{R}) \tag{17}$$

where $V^{(3)}_{EHF}(\mathbf{R})$, $V^{(3)}_{ele}(\mathbf{R})$, and $V^{(3)}_{dc}(\mathbf{R})$ are the extended Hartree−Fock, dynamic correlation, and electrostatic three-body energy contributions; for details, see ref 24. Suffice it to highlight that, as usual in a single-sheeted formalism, the $V^{(3)}_{EHF}(\mathbf{R})$ term has been employed to least-squares fit the ab initio data, hence providing a smooth DMBE PES where the cusps due to the $^2A_2/^2B_1$ crossing seam have been smoothed out. We shall refer to it as $V(\mathrm{R})$.

Because the $^2A_2/^2B_1$ crossing seam occurs near a region containing the most relevant stationary points of the $NO_2(1^2A'')$ system, the DMBE form has been modified in ref 24 by adding Gaussian terms that allow a slight improvement on the description of the cusp, with the PES assuming the form

$$V'(\mathbf{R}) = V(\mathrm{R}) + \sum_j G_{(j)}(\mathbf{R}) \tag{18}$$

and the $G_{(j)}(\mathbf{R})$ functions given by

$$G_{(j)}(\mathbf{R}) = \frac{1}{2}P_{(j)}\prod_{i=1}^{3}\exp\{\gamma_i^{(j)}[R_i - R_i^{(j,0)}]^2\} \tag{19}$$

DOI: 10.1021/jp512671q
J. Phys. Chem. A 2015, 119, 1415−1421

with $P_{(j)}$ being polynomial forms. Note that the summation in eq 18 accounts for the fact that more than one Gaussian term may be employed, in which case they can be distributed in configuration space. Such a procedure has been shown to be very effective on reducing the discrepancies between the single-sheeted $V(\mathrm{R})$ form and the ab initio data in the vicinity of crossing seam but obviously could not show any cusp due to using analytic functions.

In this work, we introduce the correct cusp behavior by writing

$$G'(\mathbf{R}) = [P_{(1)} - \Delta \cdot P_{(2)}] \prod_{i=1}^{3} \exp\{\gamma[R_i - R_i^{(0)}]^2\} \tag{20}$$

with the novel PES assuming the form

$$V''(\mathbf{R}) = V(\mathrm{R}) + G'(\mathrm{R}) \tag{21}$$

Although a single-centered term has been considered in $G'(\mathrm{R})$, a summation of distributed terms may be adopted when judged relevant. Clearly, $G'(\mathrm{R})$ plays a role similar to the term $[P_{1,-} - \Delta P_{2,-}]T(\mathbf{R})$ in eq 12. However, unlike eq 12, where $[P_{1,-} - \Delta P_{2,-}]T(\mathbf{R})$ fully accounts for the $V_{\mathrm{EHF}}(\mathbf{R})$ part of the PES, eq 20 is mostly added to mimic the cusp behavior. Moreover, $G'(\mathrm{R})$ dies-off Gaussian-like, which has the effect of restricting its influence to the region of the cusp, thus fully preserving the $V(\mathbf{R})$ attributes. Regarding $P_{(1)}$ and $P_{(2)}$ in eq 20, we have found it to be satisfactory to use the following third-order polynomial

$$\begin{aligned} P(\mathbf{Q}) = {} & c_1 + c_2Q_1 + c_3Q_3 + c_4Q_1^2 + c_5S_{2a}^2 + c_6Q_1Q_3 \\ & + c_7S_{2b}^2 + c_8Q_1^3 + c_9Q_1S_{2a}^2 + c_{10}S_3^3 + c_{11}Q_1^2Q_3 \\ & + c_{12}Q_1S_{2b}^2 + c_{13}Q_3S_{2a}^2 \end{aligned} \tag{22}$$

where $S_{2a}^2 = Q_2^2 + Q_3^2$, $S_{2b}^2 = Q_2^2 - Q_3^2$ and $S_3^3 = Q_3^3 - 3Q_2^2Q_3$. Of course, the use of more sophisticated $G'(\mathrm{R})$ forms is a matter of convenience and will not be further addressed.

The final results are shown in Figures 4 and 5 and Table 1, with the fitting parameters given in Table 2.

Note that the set of 1687 ab initio points calculated in ref 24 is reproduced with a root-mean-square deviation of rmsd ≈ 1.06 kcal mol^{-1}. Figure 3a–c shows contour plots of $V(\mathbf{R})$, $V'(\mathbf{R})$, and $V''(\mathbf{R})$ for the T-shaped N atom insertion in O_2. Despite the significant improvement in the vicinity of the $^2A_2/^2B_1$ crossing seam due to the addition of $G(R)$, $G'(R)$ is seen to not only provide a similar improvement but also display the sharp nature of the PES at that region. This can perhaps be best seen from Figure 5a–c. As shown, the sharp nature of the cusp can only be correctly described by $V''(\mathbf{R})$. In turn, Figure 5d–f shows the evolution of the cusp when one moves away from the locus of intersection. Clearly, $V''(\mathbf{R})$ provides a much better description of the cusp. In fact, recalling that the modeling of $V''(\mathbf{R})$ implies only a modest difficulty when compared with fitting $V'(\mathbf{R})$, as the former involves less than half of the number of linear coefficients, one may safely state that further improvements within the current single-sheeted formalism can be readily obtained if so desired. Far from the crossing point, all PESs are similar due to the Gaussian form of eqs 19 and 20.

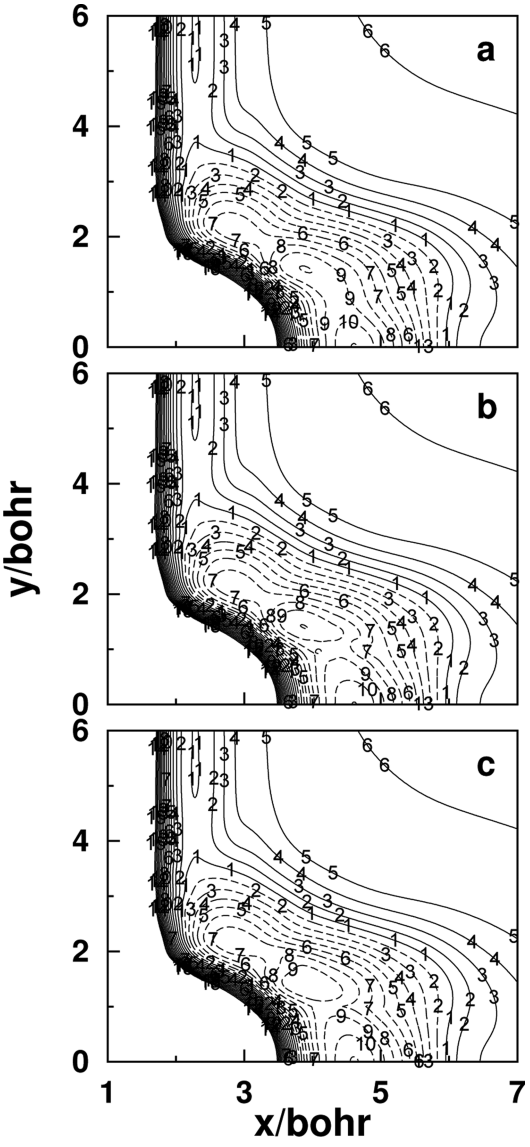

Figure 4. Isoenergy contour plots for N plus O_2 C_{2v} insertion. Contours start at the N+O_2 energy and are separated by energy intervals of $\Delta E/E_h = +0.02$ (solid lines) or $\Delta E/E_h = -0.02$ (dashed). Key for panels: (a) $V(\mathbf{R})$, (b) $V'(\mathbf{R})$, and (c) $V''(\mathbf{R})$.

PERMUTATIONALLY EQUIVALENT CROSSING SEAMS: $N_3(^2A')$

When a tritatomic system presents two or more permutationally equivalent crossings, an extra difficulty arises in applying the method. A classical example refers to the linear dissociation of H_2O, where a Σ/Π crossing occurs. Suppose that this occurs for a geometry such as $H_aO\cdots H_b$, which by swapping the hydrogen atoms gives $H_bO\cdots H_a$. If we are to apply the current approach, there would be no unique way to simultaneously define the distance of a point to both crossing seams.

To illustrate the idea, consider $N_3(^2A')$, a species of interest in atmospheric chemistry that has received considerable theoretical attention[26−31] and has recently been accurately modeled[14,32,33] using a diabatic matrix.[1] The crossing occurs now for C_{2v} symmetries with a valence angle α,[34] as shown in Figure 6, and there are three permutationally equivalent lines. Focusing on one of these lines, the crossings can be reasonably modeled in $\mathbf{R}$ space for a fixed valence angle of $\alpha = 110.3°$

DOI: 10.1021/jp512671q
J. Phys. Chem. A 2015, 119, 1415−1421

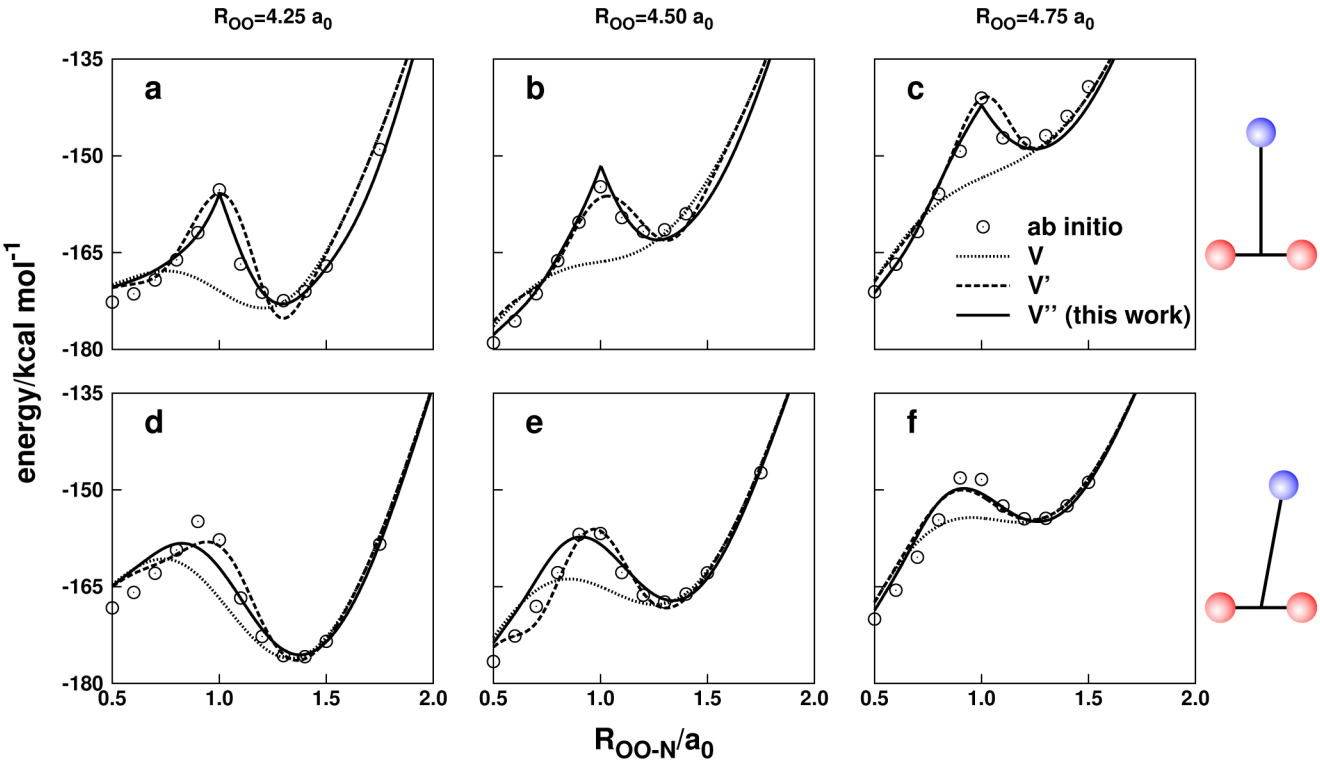

Figure 5. Profiles for N plus O_2 interactions. Upper and lower panels correspond to θ_{N-O_2} values of 90 and 80°, respectively. Energies referred to the atomization limit.

Table 1. Stationary Points of NO_2[a]

$R_{NO'}$	$R_{NO''}$	∠ONO	ω_s, ω_b, ω_a	energy[b]	potential, level of theory
			C_s distorted minimum (DM)		
2.7534	2.2197	109.67	1668, 780, 369	0.00	$V(\mathbf{R})$
2.7426	2.2227	109.65	1663, 786, 293	0.00	$V'(\mathbf{R})$
2.7561	2.2203	109.28	1602, 864, 378	0.00	$V''(\mathbf{R})$
			C_{2v} transition state (TS1)		
2.4054	2.4054	108.14	1454, 723, 45*i*	0.50	$V(\mathbf{R})$
2.3968	2.3968	107.77	1686, 698, 663*i*	0.81	$V'(\mathbf{R})$
2.4055	2.4055	110.54	1497, 777, 522*i*	1.00	$V''(\mathbf{R})$
			linear global minimum (LM)		
2.262	2.262	180.00	1171, 957, 1827	−8.95	VQZ/MRCI[25]
2.3037	2.3037	180.00	1422, 849, 2351	−11.92	$V(\mathbf{R})$
2.3050	2.3050	180.00	1397, 857, 2250	−11.73	$V'(\mathbf{R})$
2.3048	2.3048	180.00	1425, 837, 2360	−12.24	$V''(\mathbf{R})$
			pseudo-transition state (TS5)		
2.39	2.39	131.00		19.30	VQZ/MRCI[25]
2.3329	2.3329	138.08		9.73	$V(\mathbf{R})$
2.1475	2.4761	135.13		20.52	$V'(\mathbf{R})$
2.2624	2.4104	133.09		16.44	$V''(\mathbf{R})$

[a]Distances in bohr, angles in degrees, frequencies in cm^{-1}, and energies in kcal mol^{-1}. [b]Energies relative to the C_s distorted minimum.

where $R_1 = R_2 = R$, $R_3 = R(2(1 - \cos\alpha))^{1/2}$. The parametric equation for the crossing is then $(t,t,t(2(1 - \cos\alpha))^{1/2})$.[34] In turn, the distance from a point $\vec{\mathbf{p}} = (r_1,r_2,r_3)$ to the crossing seam at $\vec{\mathbf{p}}_0(t_0,t_0,t_0(2(1-\cos\alpha))^{1/2})$ is given by

$$\|\vec{\Delta}\| = \sqrt{(r_1 - t_0)^2 + (r_2 - t_0)^2 + [r_3 - t_0\sqrt{2(1 - \cos\alpha)}]^2} \quad (23)$$

with t_0 extracted from

$$\vec{\Delta}\cdot\vec{\mathbf{p}}_0 = (r_1 - t_0)t_0 + (r_2 - t_0)t_0 + [r_3 - t_0\sqrt{2(1 - \cos\alpha)}]t_0\sqrt{2(1 - \cos\alpha)} = 0 \quad (24)$$

which yields

$$t_0 = \frac{r_1 + r_2 + r_3\sqrt{2(1 - \cos\alpha)}}{4 - 2\cos\alpha} \quad (25)$$

The distance $\vec{\Delta}$ to such a crossing can then be obtained from eq 23, which allows us to create a cusp on the adiabatic PESs for the above specific crossing. However, the PES will not be

DOI: 10.1021/jp512671q
J. Phys. Chem. A 2015, 119, 1415−1421

Table 2. Optimized Parameters in Equation 20

	$P_{1,-}$	$P_{2,-}$
c_1/E_h	0.02626722	0.08861928
$c_2/a_0^{-1}E_h$	−0.04099395	−0.05862657
$c_3/a_0^{-1}E_h$	0.07137945	−0.00709396
$c_4/a_0^{-2}E_h$	0.24820100	0.28240427
$c_5/a_0^{-2}E_h$	1.03116057	0.77111966
$c_6/a_0^{-2}E_h$	−0.70347202	−0.55170094
$c_7/a_0^{-2}E_h$	0.26786311	0.01148359
$c_8/a_0^{-3}E_h$	0.01139784	0.08786851
$c_9/a_0^{-3}E_h$	0.29096697	−0.29870668
$c_{10}/a_0^{-3}E_h$	−0.81012359	−0.47670087
$c_{11}/a_0^{-3}E_h$	−0.04555723	0.15554441
$c_{12}/a_0^{-3}E_h$	−1.07408515	−0.51462827
$c_{13}/a_0^{-3}E_h$	−1.08690202	0.17021435
$R_1^{(0)}/a_0$	4.5000	4.5000
$R_2^{(0)}/a_0$	2.4233	2.4233
$R_3^{(0)}/a_0$	2.4233	2.4233
γ_1/a_0^{-1}	1.90	1.90
γ_2/a_0^{-1}	10.40	10.40
γ_3/a_0^{-1}	10.40	10.40

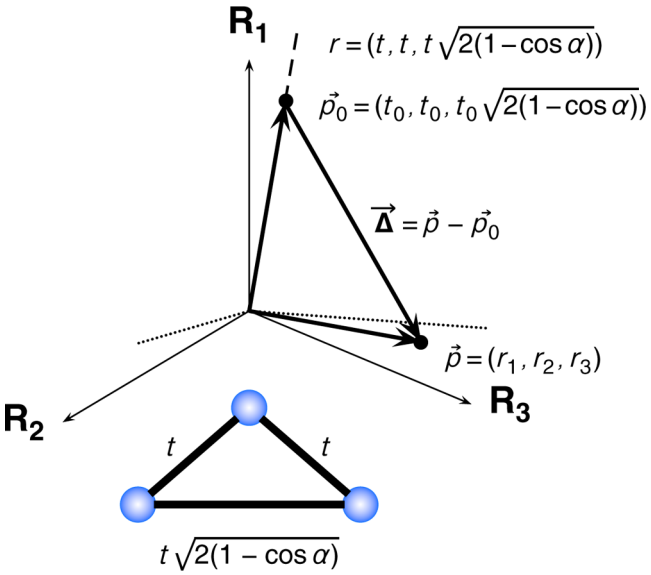

Figure 6. C_{2v} crossing seam of $N_3(^2A')$ (dashed line) and the two other equivalent seams (dotted).

permutationally symmetric as it should, with other crossing seams unattended. We solve this problem by calculating the distance from the point (r_1, r_2, r_3) to the three crossings ($\vec{\Delta}_1$, $\vec{\Delta}_2$, and $\vec{\Delta}_3$), and writing

$$V_{\pm} = V_{\pm}^{(2)} + V_{dc}^{(3)} + P_{\pm}^{(3)} \times T_1(\mathbf{R}) \pm \Delta_1\Delta_2\Delta_3 \times T_2(\mathbf{R}) \quad (26)$$

where $T_1(\mathbf{R})$ and $T_2(\mathbf{R})$ are range-decaying functions that vanish in the desired regions. $T_2(\mathbf{R})$ is perhaps best chosen to be a Gaussian centered at each of the minima of the crossing seam, thus avoiding any impact at regions far from the crossing

$$T_2(\mathbf{R}) = \exp(-(R_1 - 2.40)^2 - (R_2 - 2.40)^2 - (R_3 - 3.94)^2) \quad (27)$$

$$+ \exp(-(R_1 - 2.40)^2 - (R_2 - 3.94)^2 - (R_3 - 2.40)^2) \quad (28)$$

$$+ \exp(-(R_1 - 3.94)^2 - (R_2 - 2.40)^2 - (R_3 - 2.40)^2) \quad (29)$$

We have applied this to the modeling of both the ground and excited $^2A'$ states of N_3, which is presented in Figure 7. As

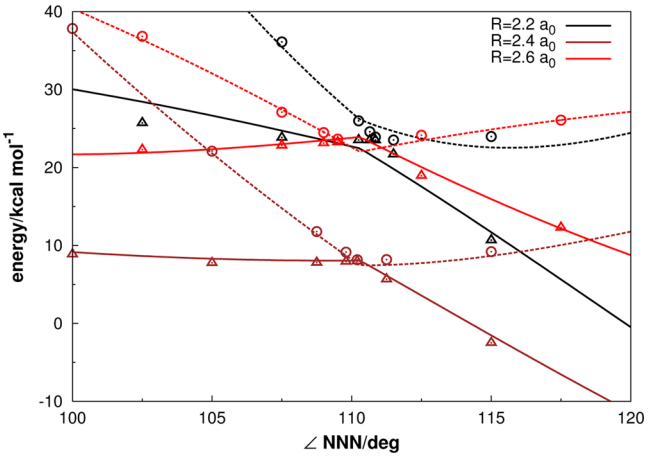

Figure 7. Potential energy profile for the C_{2v} bend of the $N_3(^2A')$. The ab initio energies are given by the points, and the fits using eq 26 are shown by the lines (solid line for the ground state, dashed line for the upper one.).

shown, we have successfully included a cusp on the ground and excited states without any polynomials multiplied by the $\vec{\Delta}$ terms, but the proper degeneracy cannot be guaranteed by the model. To ensure degeneracy, one must devise a new basis for the polynomials, with independent monomers capable of vanishing at all crossing seams. Because there is already a high-level diabatic potential matrix for this system,[33] which does ensure the required degeneracies of the adiabatic PESs at the crossing seam, no attempt to construct a better version is here attempted. In the future, however, instead of the overly complex task of diabatizing the ab initio energies and fitting the whole matrix, one could simply employ the approach given in this work to obtain such an accurate representation.

CONCLUDING REMARKS

We have suggested a simple scheme to generate PESs capable of fitting the seams due to any conical intersections. It can be of great utility when modeling PESs for reaction dynamics because the fit with a smooth function gets very problematic in such regions. The method requires only a geometrical description of the crossing seam and hence is easy to use. The fit of crossing seams in larger polyatomics is a complicated issue that requires proper examination irrespective of the approach used and hence is beyond the scope of the present work.

AUTHOR INFORMATION

Corresponding Authors

*B.R.L.G.: E-mail: brenogalvao@gmail.com.
*V.C.M.: E-mail: vinicius.c.mota@ufes.br.
*A.J.C.V.: E-mail: varandas@uc.pt.

Notes

The authors declare no competing financial interest.

ACKNOWLEDGMENTS

This work has the support of Fundação para a Ciência e a Tecnologia, Portugal, under contracts PTDC/CEQ-COM3249/2012 and PTDC/AAG-MAA/4657/2012 as well as the support for the Coimbra Chemistry Centre through the

DOI: 10.1021/jp512671q
J. Phys. Chem. A 2015, 119, 1415−1421

project PEst-OE/QUI/UI0313/2014. Support from the Brazilian funding agency Coordenação de Aperfeiçoamento de Pessoal de Nível Superior (CAPES) is further acknowledged.

REFERENCES

(1) Mota, V. C.; Varandas, A. J. C. $HN_2(^2A')$ Electronic Manifold. II. Ab Initio Based Double-Sheeted DMBE Potential Energy Surface via a Global Diabatization Angle. *J. Phys. Chem. A* **2008**, *112*, 3768−3786.
(2) Yang, K. R.; Xu, X.; Truhlar, D. G. Direct Diabatization of Electronic States by the Fourfold-Way: Including Dynamical Correlation by Multi-Configuration Quasidegenerate Perturbation Theory with Complete Active Space Self-Consistent-Field Diabatic Molecular Orbitals. *Chem. Phys. Lett.* **2013**, *573*, 84−89.
(3) Varandas, A. J. C.; Brown, F. B.; Mead, C. A.; Truhlar, D. G.; Blais, N. C. A Double Many-Body Expansion of the Two Lowest-Energy Potential Surfaces and Nonadiabatic Coupling for H_3. *J. Chem. Phys.* **1987**, *86*, 6258−6269.
(4) London, F. Quantenmechanische Deutung Des Vorgangs Der Aktivierung. *Z. Electrochem.* **1929**, *35*, 552−555.
(5) Eyring, H.; Polanyi, M. Uber Einfache Gasreaktionen. *Z. Phys. Chem. B* **1931**, *12*, 279−311.
(6) Sato, S. Potential Energy Surface of the System of 3 Atoms. *J. Chem. Phys.* **1955**, *23*, 2465−2466.
(7) Ellison, F. O. A Method of Diatomics in Molecules. I. General Theory and Application to H_2O. *J. Am. Chem. Soc.* **1963**, *85*, 3540−3544.
(8) Tully, J. C. Semiempirical Diatomics-in-Molecules Potential Energy Surfaces. *Adv. Chem. Phys.* **1980**, *42*, 63−112.
(9) Kuntz, P. J. Interaction Potentials II. Semiempirical Atom-Molecule Potentials for Collision Theory. In *Atom−Molecule Collision Theory*; Bernstein, R., Ed.; Plenum: New York, 1979; p 79.
(10) Mead, C. A.; Truhlar, D. G. Conditions for the Definition of a Strictly Diabatic Electronic Basis for Molecular-Systems. *J. Chem. Phys.* **1982**, *77*, 6090−6098.
(11) Porter, R. N.; Stevens, R. M.; Karplus, M. Symmetric H_3: A Semiempirical and Ab Initio Study of a Simple Jahn-Teller System. *J. Chem. Phys.* **1968**, *49*, 5163−5178.
(12) Murrell, J. N.; Sorbie, K. S.; Varandas, A. J. C. Analytical Potential of Triatomic Molecules from Spectroscopic Data II. Application to Ozone. *Mol. Phys.* **1976**, *32*, 1359−1372.
(13) Varandas, A. J. C.; Murrell, J. N. Many-body Expansion of Polyatomic Potential-Energy Surfaces: Application to H_n Systems. *Faraday Discuss. Chem. Soc.* **1977**, *62*, 92−109.
(14) Galvão, B. R. L.; Varandas, A. J. C. Ab Initio Based Double-Sheeted DMBE Potential Energy Surface for $N_3(^2A'')$ and Exploratory Dynamics Calculations. *J. Phys. Chem. A* **2011**, *115*, 12390−12398.
(15) Weyl, H. *The Classical Theory of Groups*; Princeton University Press: Princeton, NJ, 1946.
(16) Murrell, J. N.; Carter, S.; Farantos, S. C.; Huxley, P.; Varandas, A. J. C. *Molecular Potential Energy Functions*; Wiley: Chichester, U.K., 1984.
(17) Varandas, A. J. C.; Alijah, A.; Cernei, M. A Novel Accurate Representation of a Double-Valued Potential Energy Surface by the DMBE Method. Application to Triplet H_3^+ (a^3E'). *Chem. Phys.* **2005**, *308*, 285−295.
(18) Varandas, A. J. C. A Double Many-Body Expansion of Molecular Potential Energy Functions. I. Hartree-Fock-Approximate Correlation Energy (HFACE) Potential for the Helium-Hydrogen (HeH_2) van der Waals Molecule. *Mol. Phys.* **1984**, *53*, 1303−1325.
(19) Varandas, A. J. C. Intermolecular and Intramolecular Potentials: Topographical Aspects, Calculation, and Functional Representation via a DMBE Expansion Method. *Adv. Chem. Phys.* **1988**, *74*, 255−338.
(20) Varandas, A. J. C. Modeling and Interpolation of Global Multi-Sheeted Potential Energy Surfaces. In *Conical Intersections: Electronic Structure, Dynamics & Spectroscopy*; Domcke, W., Yarkony, D. R., Köppel, H., Eds.; Advanced Series in Physical Chemistry; World Scientific Publishing: River Edge, NJ, 2004; Vol. *15*, p 205, Chapter 5.
(21) Varandas, A. J. C. Combined-Hyperbolic-Inverse-Power-Representation of Potential Energy Surfaces: A Preliminary Assessment for H_3 and HO_2. *J. Chem. Phys.* **2013**, *138*, 054120.
(22) Varandas, A. J. C. Putting Together the Pieces: Global Description of Valence and Long-Range Forces via Combined Hyperbolic Inverse-Power Representation of the Potential Energy Surface for Use in Reaction Dynamics. In *Reaction Rate Constant Computations: Theories and Applications*; Han, K., Chu, T., Eds.; The Royal Society of Chemistry: Cambridge, U.K., 2014; Vol. *17*, pp 408−445.
(23) Mota, V. C.; Caridade, P. J. S. B.; Varandas, A. J. C. Toward the Modeling of the $NO_2(^2A'')$ Manifold. *Int. J. Quantum Chem.* **2011**, *111*, 3776−3785.
(24) Mota, V. C.; Varandas, A. J. C. Ab Initio-Based Global Double Many-Body Expansion Potential Energy Surface for the First $^2A''$ Electronic State of NO_2. *J. Phys. Chem. A* **2012**, *116*, 3023−3034.
(25) Ivanov, M. V.; Zhu, H.; Schinke, R. Theoretical Investigation of Exchange and Recombination Reactions in $O(^3P)$ + NO Collisions. *J. Chem. Phys.* **2007**, *126*, 054304.
(26) Wang, D.; Stallcop, J. R.; Huo, W. M.; Dateo, C. E.; Schwenke, D. W.; Partridge, H. Quantal Study of the Exchange Reaction for N + N_2 Using an Ab Initio Potential Energy Surface. *J. Chem. Phys.* **2003**, *118*, 2186−2189.
(27) Zhang, P.; Morokuma, K.; Wodtke, A. M. High-level Ab Initio Studies of Unimolecular Dissociation of the Ground-State N_3 Radical. *J. Chem. Phys.* **2005**, *122*, 014106.
(28) Caridade, P. J. S. B.; Galvão, B. R. L.; Varandas, A. J. C. Quasiclassical Trajectory Study of Atom-Exchange and Vibrational Relaxation Processes in Collisions of Atomic and Molecular Nitrogen. *J. Phys. Chem. A* **2010**, *114*, 6063−6070.
(29) Galvão, B. R. L.; Varandas, A. J. C.; Braga, J. P.; Belchior, J. C. Vibrational Energy Transfer in $N(^2D)$ + N_2 Collisions: A Quasiclassical Trajectory Study. *Chem. Phys. Lett.* **2013**, *577*, 27−31.
(30) Galvão, B. R. L.; Varandas, A. J. C.; Braga, J. P.; Belchior, J. C. Electronic Quenching of $N(^2D)$ by N_2: Theoretical Predictions, Comparison with Experimental Rate Constants, and Impact on Atmospheric Modeling. *J. Phys. Chem. Lett.* **2013**, *4*, 2292−2297.
(31) Galvão, B. R. L.; Varandas, A. J. C.; Braga, J. P.; Belchior, J. C. Electronic Quenching in $N(^2D')$ + N_2 Collisions: A State-Specific Analysis via Surface Hopping Dynamics. *J. Chem. Theory Comput.* **2014**, *10*, 1872−1877.
(32) Galvão, B. R. L.; Varandas, A. J. C. Accurate Double Many-Body Expansion Potential Energy Surface for N_3 from Correlation Scaled Ab Initio Energies with Extrapolation to the Complete Basis Set Limit. *J. Phys. Chem. A* **2009**, *113*, 14424−14430.
(33) Galvão, B. R. L.; Caridade, P. J. S. B.; Varandas, A. J. C. $N(^4S/^2D)$+N_2: Accurate Ab Initio-Based DMBE Potential Energy Surfaces and Surface-Hopping Dynamics. *J. Chem. Phys.* **2012**, *137*, 22A515.
(34) Wang, Z.; Kerkines, I. S. K.; Morokuma, K.; Zhang, P. Analytical Potential Energy Surfaces for N_3 Low-Lying Doublet States. *J. Chem. Phys.* **2009**, *130*, 044313.

DOI: 10.1021/jp512671q
J. Phys. Chem. A 2015, 119, 1415−1421